Research article

Integrated analysis of purine metabolism assists in predicting prognosis and treatment decisions for patients with lung adenocarcinoma

Tingting Zhang [a], Ruhua Chen [a], Xiangyu Su [b], Meng Wang [a], Qin Lu [a,*]

[a] *Department of Respiratory and Critical Care Medicine, Yixing Hospital Affiliated to Jiangsu University, Wuxi, 214221, China*
[b] *Department of Oncology, Zhongda Hospital, School of Medicine, Southeast University, Nanjing, 21009, China*

A B S T R A C T

The incidence of lung cancer, especially lung adenocarcinoma (LUAD), has recently increased. Targeted therapy and immunotherapy combined with conventional treatment have shown surprising benefits in enhancing the LUAD patient's prognosis. For the purpose of guiding treatment planning and the prognosis of LUAD, more research is required. The particular aim of this work was to establish a purine metabolism scoring (PMS) model for the purpose of individually forecasting treatment outcomes and overall survival for patients who have LUAD. Clinical and whole genome data were obtained from the TCGA-LUAD cohort via "UCSC". The 25 driver purine metabolism-related prognostic genes were determined founded on univariate Cox regression. Then PMS was developed through stepwise LASSO Cox regression. Survival analysis indicated that patients who have PMS experienced worse outcomes. We validated the PGM2 effect on lung adenocarcinoma malignancy in in vitro experiments. Univariate as well as multivariate Cox regression suggested that PMS was an independent prognostic indicator for LUAD patients, which was confirmed in subgroup analysis. Functional assay demonstrated that immune response as well as cytotoxicity pathways have a connection with lower PMS, and patients who have low PMS possess an active immune microenvironment. Moreover, the LUAD patients who have low PMS showed greater sensitivity to immunotherapy, targeted therapy, as well as chemotherapy. Knockdown of PGM2 was discovered to decrease the proliferation, invasion, as well as migration of lung adenocarcinoma cells in an in vitro assay. Pertaining to this particular research, we created a PMS model and conducted a thorough analysis of purine metabolism in LUAD in order to determine prognosis and offer recommendations for treatment. This finding offered a fresh concept for the clinical management of LUAD and novel therapy protocols.

1. Introduction

Among the most prevailing malignant tumors in the respiratory system is lung cancer, and there is an increasing trend in the lung cancer's incidence, making it rank the most frequent cancer [1,2]. In worldwide, the majority of lung cancer patients (70%) was identified as having lung adenocarcinoma (LUAD) [3]. Patients with LUAD usually had an inferior prognosis since the advanced LUAD 5-year survival rate is below 20% [4,5]. When patients have unresectable advanced LUAD, chemotherapy as well as radiotherapy are

---

the cornerstones [6]. In addition, the past few decades have seen the growth of targeted therapies and/or immunotherapy-based combined therapies for LUAD patients [7]. However, response to treatment varies among patients individually, and novel biomarkers are needed to aid prognosis and determine the optimal regimens.

Purine metabolism is crucial in cancer progression and has a close connection to the growth, metastasis, as well as efficacy of therapies for tumors [8]. As one of the basic components of DNA molecules, purines is vital in DNA synthesis and maintenance in cancer cells, and thus tumor cells require large amounts of purine nucleotides to support their rapid cell division and proliferation [9]. Adenosine to inosine ratio imbalance often occurs in the cancer process, and the disturbance of purine metabolism is largely involved in tumor growth, invasion, as well as metastasis [10]. Additionally, purines are involved in the regulation of immune cell activity as well as cytokine release via different receptors and receptor subtypes, affecting anti-tumor immune effects [11]. In the last few years, adenosine metabolism has become an emerging concept in cancer research, and adenosine synthesized from adenine is considered to be an important factor in regulating the immune escape of tumor cells [12,13]. Targeting purine metabolism is expected to assist immunotherapy [13]. Antimetabolites targeting purines, such as methotrexate, were the first classical anticancer drugs developed and are widely used in clinical treatment [14]. Therefore, targeting purine metabolism represents a potentially successful area for cancer treatment, and further studies on novel regulatory mechanisms of purine metabolism in cancer immunotherapy are needed to provide new ideas for existing cancer immunotherapy.

Pertaining to this particular research, we integrated LUAD transcriptomic data from TCGA as well as GEO with clinical data. The possible crosstalk between purine metabolism and lung cancer was systematically analyzed to explore their prognostic significance, biological heterogeneity, and possibility of using them in a clinical setting. Moreover, our study highlights the association between purine metabolism in LUAD and increases the understanding of the biological role of purine metabolism. Finally, our data may suggest that assessing the crosstalk between purine metabolism is expected to provide guidance for prognosis and treatment strategies for LUAD.

2. Methods

2.1. Data collection

We collected transcriptomic RNA-seq data, somatic variant data from maf files on the Muctect 2 platform, as well as copy number variant (CNV) data from the UCSC Xena (https://xena.ucsc.edu/) database for the TCGA-LUAD cohort. Corresponding clinical follow-up information was as well collected. After including patients having pathological typing as LUAD and excluding those with incomplete follow-up information, a TCGA-LUAD cohort of 492 LUAD patients was obtained and used as the training cohort. In addition, a large meta-GEO LUAD cohort, including GSE30219, GSE42127, and GSE7209 was collected from the GEO database. The follow-up information of patients was collected from the original supplemental material, and there were 615 patients with LUAD in total after excluding those with incomplete follow-up information. The GEO-LUAD cohort was used for external validation. 171 purine metabolism-associated genes were gathered from the MSigDB database (http://www.gsea-msigdb.org/). A comprehensive list of genes was presented in Table S1.

2.2. Construction of a purine metabolism score

Firstly, we conducted a univariate cox regression analysis for purine metabolism-related genes to identify independent prognostic factors of LUAD. Subsequently, stepwise multi-factor Cox regression was utilize to develop the purine metabolism score (PMS). The C-index of the PMS was determined via the "survcomp" package to assess prognostic efficacy [15]. A higher C-index represents a more optimal and stable prediction of the model. High PMS and low PMS groups were distinguished by the median PMS. Meanwhile, using time-dependent ROC (tROC) curves, univariate and multifactorial Cox regression, as well as Kaplan-Meier survival analysis, the independent prognostic value of PMS was thoroughly examined. In order to more accurately assess each patient's chance of survival, we built a nomogram as per PMS and clinical variables.

2.3. Cell proliferation detection

Human esophageal cancer cell lines Eca-09 and TE-1 were purchased from Bioss, China. In this study, LipofectamineTM 2000 Transfection Reagent (Invitrogen, USA) was employed for the siRNA transfection. The proliferation level of ESCA cells was detected by Cell Counting Kit-8 kit (Bioss, China). The digested single-cell solution was inoculated in 96-well plates at approximately 1500 cells per well. At 0, 12, 24, 48, and 72 h, three wells of each group were selected randomly and 10 μL of the Cell Counting Kit-8 reagent was incorporated, and the incubation came next at 37 degrPMS for 2 h. Detection of absorbance values were at 450 nm.

2.4. Analysis of potential biological regulation

To find more differentially expressed genes (DEGs) between high as well as low PMS groups, the "limma" package has been utilized. Fold change>2 as well as FDR<0.05 were the threshold values that were set. The biological functions enriched by DEGs were analyzed on the Metascape website (https://metascape.org/). In addition, we identified differential enrichment KEGG pathways between high as well as low PMS groups by GSEA software (version 4.3.1).

2.5. Evaluation of immune heterogeneity between subgroups

We measured the relative abundance concerning 22 immune cell types in individual LUAD samples via the "CIBERSORT" algorithm [16]. The "ESTIMATE" algorithm measured the samples' immune score as well as tumor purity [17]. Subsequently, we assessed the activity of the immune pathways of interest by the ssGSEA algorithm of the "GSVA" package. Finally, we examined the differences in subgroup expression of seven classical immune checkpoints.

2.6. Dissecting genomic alterations between subgroups

By utilizing the "maftools" package, the maf files were processed, and the number of nonsynonymous mutations for each patient was determined [18]. Subsequently, we analyzed the differences in high-frequency mutated genes (mutation number greater than 5) between subgroups. Additionally, we extracted significant mutation signatures for various subgroups from the maf files using the "Sigminer" package, and perform comparison of the mutation signatures with the COSMIC database [19]. Lastly, CNV data was processed using Gistic2.0, which counted deletions and amplicons based on a 0.2 threshold. For the visualization, the "ggplot2″ package was utilized.

2.7. Evaluations of chemotherapy implementation for PMS

The individual patients' sensitivity to five drugs frequently employed in LUAD (5-FU, Cisplatin, Docetaxel, Doxorubicin, and Paclitaxel) was first predicted using "pRRophetic" based on the GDSC database [20]. Ridge regression was used to estimate the IC50 values; lower IC50 values denoted greater sensitivity. Due to the fact that the genes that differed between the high as well as low PMS subgroups were assumed to be potential therapeutic targets, we uploaded the Top 150 genes that were up- and down-regulated to the CMap database (https://clue.io/) in order to look into possible small molecule compounds. In addition to predicting medications that relies on gene expression profiles, it can also reveal the biomolecular pathways targeted by drugs. Finally, the Pubmed database (https://pubmed.ncbi.nlm.nih.gov/) was employed to obtain the compounds' molecular structures that were identified.

2.8. Predicting immunotherapy response

Utilizing the genetic profiles of various immune cell phenotypes, we computed the Immunophenoscore (IPS) of the patients [21]. An active immune response and a better response to immunotherapy are indicated by a higher IPS. To anticipate the therapeutic effect of immune checkpoint blockers on individual patients, we utilized the TIDE algorithm to simulate the mechanism of tumor immune escape [22]. Furthermore, we gathered data from the well-established immunotherapy cohort Imvigor210, which included 298 patients who acquired anti-PD-L1 immunotherapy for uroepithelial cancer and had full follow-up records. The transcriptomic data from the Imvigor210 cohort were used to construct PMS based on the same method to evaluate the PMS's ability to predict immunotherapy outcomes.

2.9. Cell culture and siRNA transfection

Procell (Wuhan, China) provided the human lung cancer cell lines H1975 and A549. These cell lines were cultured in DMEM medium obtained from Bological (Israel), and maintained in a CO2-filled constant temperature incubator at 37 °C. 10% heat-inactivated fetal bovine serum (FBS) in addition to 1% penicillin were added to the DMEM medium. As directed by the manufacturer, the Lipo3000 kit from Invitrogen (USA) was utilized for transiently transfecting siRNA designed to specifically target PGM2, resulting in a temporary reduction in the target gene expression. Following transfection, the cells were cultured for 48 h and subsequently subjected to qRT-PCR analysis to assess the transcription-level silencing effect of PGM2.

2.10. Detection of cell proliferation level

A colony formation experiment was conducted to investigate the impact of knocking down PGM2 on LUAD cell lines' proliferation ability. After 48 h of cultivation, single-cell suspension was collected and seeded with approximately 1000 cells in each well of a 6-well plate. The cells were cultured in a standard DMEM medium and the medium was replaced every three days. After the formation of typical colonies was observed, LUAD cells were counted using microscopic images after being fixed with 4% formaldehyde and stained with crystal violet.

2.11. Cell invasion and migration ability detection

Transwell experiments were conducted on two types of LUAD cells: PGM2 knockdown cells and control cells, to evaluate their invasiveness and migratory capabilities. Matrigel was applied to the Transwell assay plate wells to measure invasion, while the wells without Matrigel were used for assessing migration. The number of invading cells was determined via ImageJ software. Once the fusion rate of H1975 and A549 cells reached 90%, they were collected and subjected to a 24-h starvation period in serum-free DMEM medium. A deliberate scratch was made on the starved cells using a 200 μl pipette tip, followed by washing with warm serum-free medium to eliminate cellular debris. After 48 h, the extent of wound healing at the scratch was evaluated under a microscope, and the wound

healing ratio was determined using ImageJ software to assess the cells' migratory capacity.

2.12. Bioinformatics and statistical analysis

Fisher's exact test was employed to identify variations in proportions. On top of that, the Wilcoxon test was employed to evaluate group differences in addition to the Kaplan-Meier plotter was utilized to create survival curves. Moreover, the log-rank test was used to evaluate differences in survival. Meanwhile, the R package "survivalROC" was utilized to plot time-dependent ROC curves (tROC). Via the "survival" R package, univariate and multivariate Cox regressions were conducted. Moreover, plotting nomogram and calibration curves was done via the "rms" R package. Next, the "pROC" R package was employed to examine the predictive ability of various indicators on the immunotherapy response. A two-tailed p-value of less than 0.05 was deemed significant unless otherwise stated. R software (Version 4.1.0) has been employed for each analysis.

3. Results

3.1. Dissecting key purine metabolism genes in LUAD

A total of 51 purine metabolism genes were identified as per a threshold of P less than 0.05, we demonstrated the top 25 prognostic purine metabolism genes (Fig. 1A). These 51 genes were the subject of a correlation network construction, and the findings showed a positive correlation between them (refer to Fig. 1B). Fig. 1C displays the mutation landscape of these 51 genes in the TCGA-LUAD cohort. PDE10A and PDE11A are the genes with the highest frequency of mutations. It has been discovered that missense mutations are the most common type. Lastly, we compiled a summary of the 51 important genes' CNV events (refer to Fig. 1D). The findings demonstrated that most genes had extensive CNV, with NT5C3A, POLR2K, and TWISTNV having the highest amplification frequency and AK9 and ENTPD3 having the highest deletion frequency.

3.2. Construction of the purine metabolism score

We then performed stepwise LASSO regression using these 25 genes and finally identified the best 2-gene model (PGM2 and RRM2) (Fig. 2A). We developed the PMS model following the formula: PMS = 0.003858*EXP(PGM2) + 0.001776*EXP(RRM2). C-index showed that PMS had excellent performance in the TCGA cohort and average effect in the GEO cohort (Fig. 2B). Survival analysis indicated that patients who have high PMS group suffered inferior outcomes than its competitor in different LUAD cohorts (Fig. 2C and

Fig. 1. Identification of EMT and Exosome related genes in TCGA-ESCA (A) Univariate Cox regression identified 51 purine metabolism genes with prognostic efficacy. (B) The correlation network of 51 purine metabolism genes. (C) The summary of somatic mutation of 51 purine metabolism genes. (D) The summary of CNV status of 51 purine metabolism genes.

Fig. 2. Prognostic efficacy of the purine metabolism genes score (PMS) (A) The 2-gene PMS model obtained by optimal lambda value convergence. (B) C-index comparing PMS with clinical characteristics in both TCGA and GEO cohort. (C) KM survival curves of patients with high PMS and low PMS in TCGA cohort. (D) KM survival curves of patients with high PMS and low PMS in GEO cohort. (E) The tROC curves of PMS in the GEO cohort. (G) ROC curves of PMS at 1, 3 and 5 years in the TCGA cohort. (H) ROC curves of PMS at 1, 3 and 5 years in the GEO cohort.

D). The tROC curves confirmed that the PMS is an effective predictor for OS in 5 years (Fig. 2E and F). ROC analysis revealed that PMS performed better than the other cohort in the TCGA (ROC>0.6, Fig. 2G), although the GEO cohort also showed positive results (ROC>0.6, Fig. 2H).

3.3. Evaluation of the predictive independence of PMS

We initially analyzed the relationship between PMS and patient clinical characteristics (which includes gender, age as well as stage) via one-way Cox and multifactor Cox regression. In both the training and validation sets, PMS was discovered to be an independent prognostic indicator (P < 0.05) by one-factor Cox regression (Fig. 3A). PMS persisted as an unfavorable factor for OS in the training as well as validation cohorts, as determined by multi-factor Cox regression (P < 0.05) (Fig. 3B). Therefore, in patients with LUAD, PMS may be a reliable prognostic indicator for OS. Then, we created a Nomogram to more accurately measure the risk evaluation of LUAD patients (Fig. 3C). The Nomogram's curve demonstrated good accuracy and stability at one, three, and five years (Fig. 3D). The tROC analysis shows that the Nomogram model possesses a better performance compared to use PMS alone. (Fig. 3E).

3.4. Dissecting the biological background of PMS

To examine the biological characteristics associated with PMS in LUAD, we first identified DEGs between low and high PMS groups via the limma algorithm. By functional enrichment, we discovered that genes upregulated in high PMS were associated with the
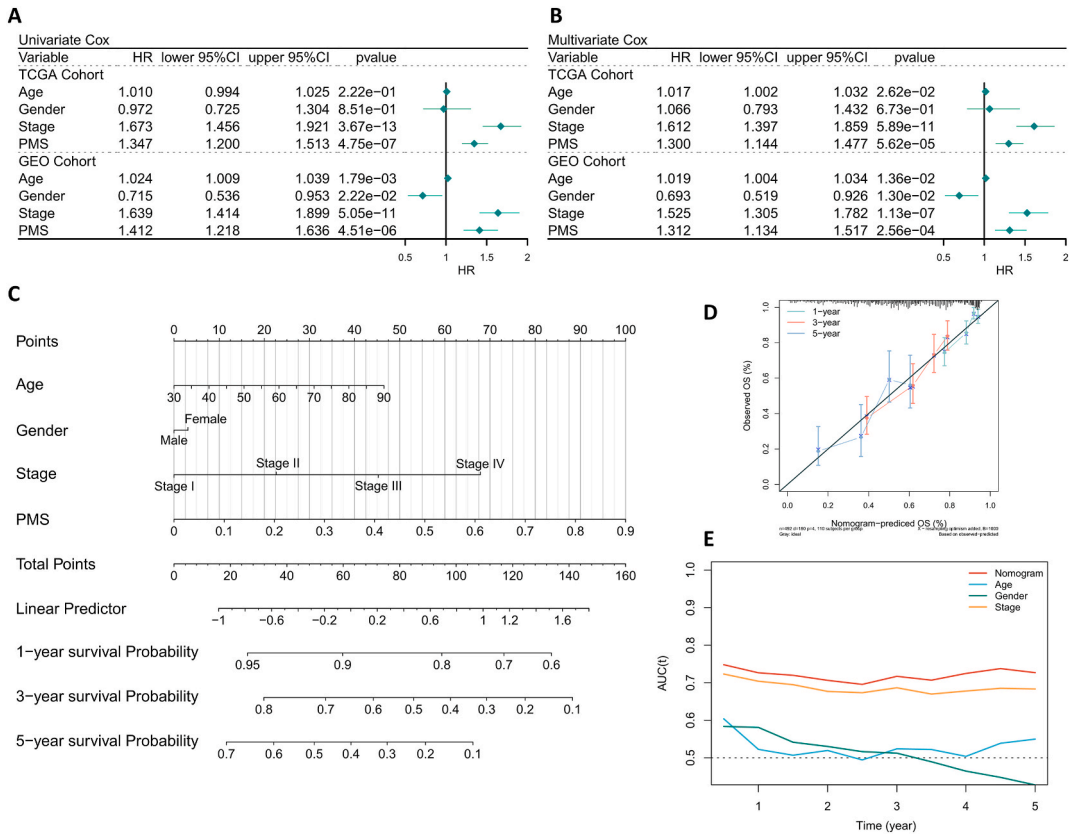
Fig. 3. Verifying the independence and robustness of PMS (A) Univariate COX regression analysis of OS in TCGA and GEO datasets. (B) Multivariate COX regression analysis of OS in TCGA and GEO datasets. (C) The subgroup analysis of PMS in the whole cohort. (D) Nomogram based on PMS and clinical characteristics. (E) Calibration curve of Nomogram. (F) tROC curve of Nomogram and clinical characteristics.
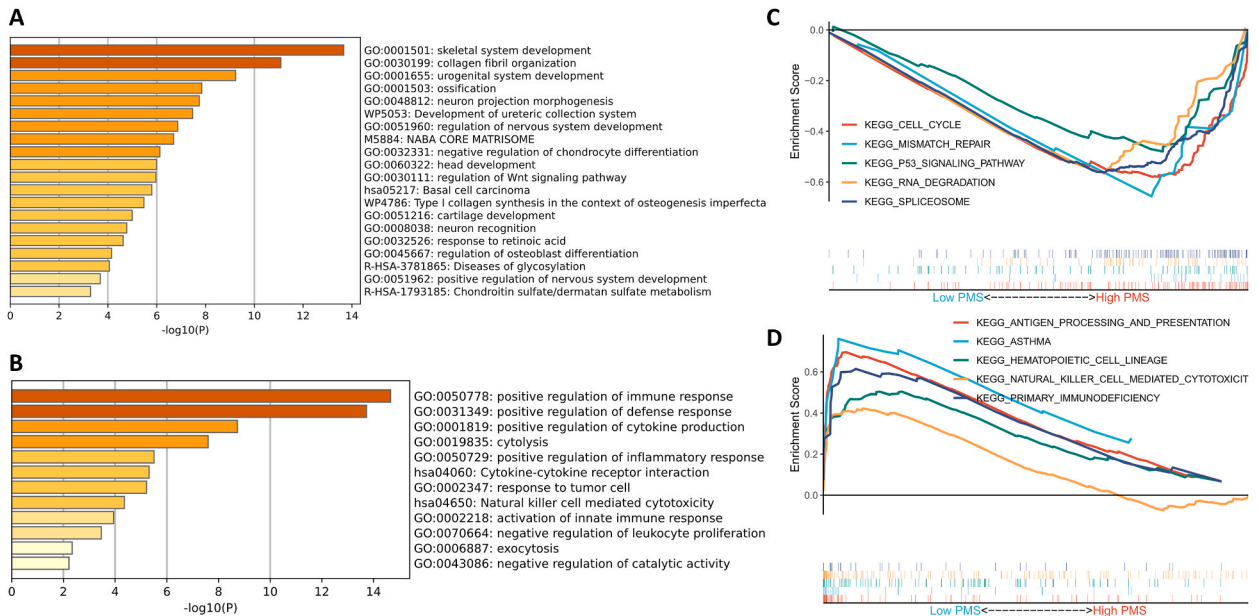
Fig. 4. Dissecting the biological and functional background of PMS (A) Functional enrichment of characteristic genes in the high PMS group. (B) Functional enrichment of characteristic genes in the low PMS group. (C) The top 5 KEGG pathways enriched in the high PMS group. (D) Top 5 KEGG pathways enriched in the low PMS group.

cytoskeleton, collagen fibers, and WNT signaling pathway (Fig. 4A). Conversely, the genes that were upregulated in low PMS were linked to cytolysis, immune response, and cytokine (Fig. 4B). Further GSEA and KEGG analysis indicated that the genes linked to the cell cycle, P53 signaling pathway, RNA degradation, as well as other replication dysregulation-related pathways were upregulated in the high PMS group (Fig. 4C). Based on this, we infer that high PMS tumors proliferate and migrate mainly through active skeletal response and collagen fibrils through the extracellular matrix. On the other hand, low PMS tumors have an active anti-tumor immune response, as antigen presentation, cytotoxicity, as well as hematopoietic cell lineage were upregulated (Fig. 4D).
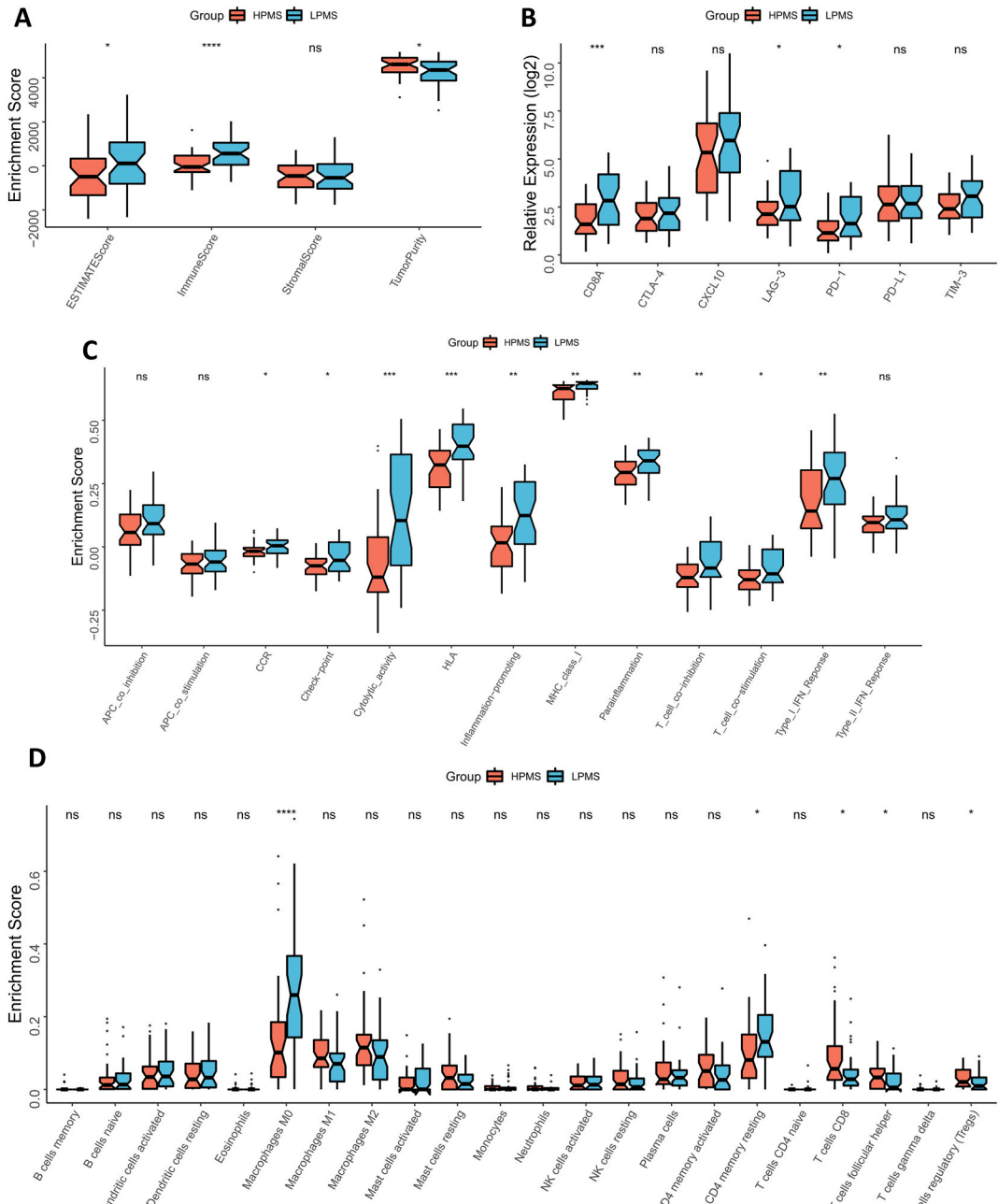
Fig. 5. Dissecting the immune microenvironment of different PMS groups (A) Differences in Estimate scores between the high and low PMS groups in the TCGA-ESCA cohort. (B) Differences in expression level of classical immune checkpoint between high and low PMS groups in the TCGA-LUAD cohort. (C) Differences in immune-related pathway activity between high and low PMS groups in the TCGA-LUAD cohort. (D) Differences in immune cell infiltration between the high and low PMS groups in the TCGA-LUAD cohort.

3.5. Low PMS and abundant immune infiltration associated

Next, we examined PMS's tumor immune microenvironment. Even though the group with low PMS had higher immune and estimate scores, the ESTIMATE results specified higher tumor purity in the high PMS group (Fig. 5A). Furthermore, we found elevated expression of CD8A, LAG-3, and PD-1 in low PMS (Fig. 5B). Using ssGSEA, we then evaluated immune-related pathways' activity. The low PMS group was found to have a significant enrichment in most immune-related pathways, in accordance to the findings (Fig. 5C). In conclusion, we discovered that the low PMS group possessed more M0 macrophages and CD4 T cells, while the high PMS group had more gamma delta T cells, CD8 T cells, as well as Tregs infiltrate (Fig. 5D). Therefore, we hypothesized that Tregs suppressed the antitumor immune response in the high PMS group, whereas the low PMS immune infiltration was elevated.

3.6. Correlation of PMS with genomic alterations

Afterward, we examined the TCGA-LUAD genome-wide data to interpret the status of genomic alterations in various PMS groups. We discovered a significant positive correlation between PMS and TMB, with significantly upregulated TMB observed in LUAD patients
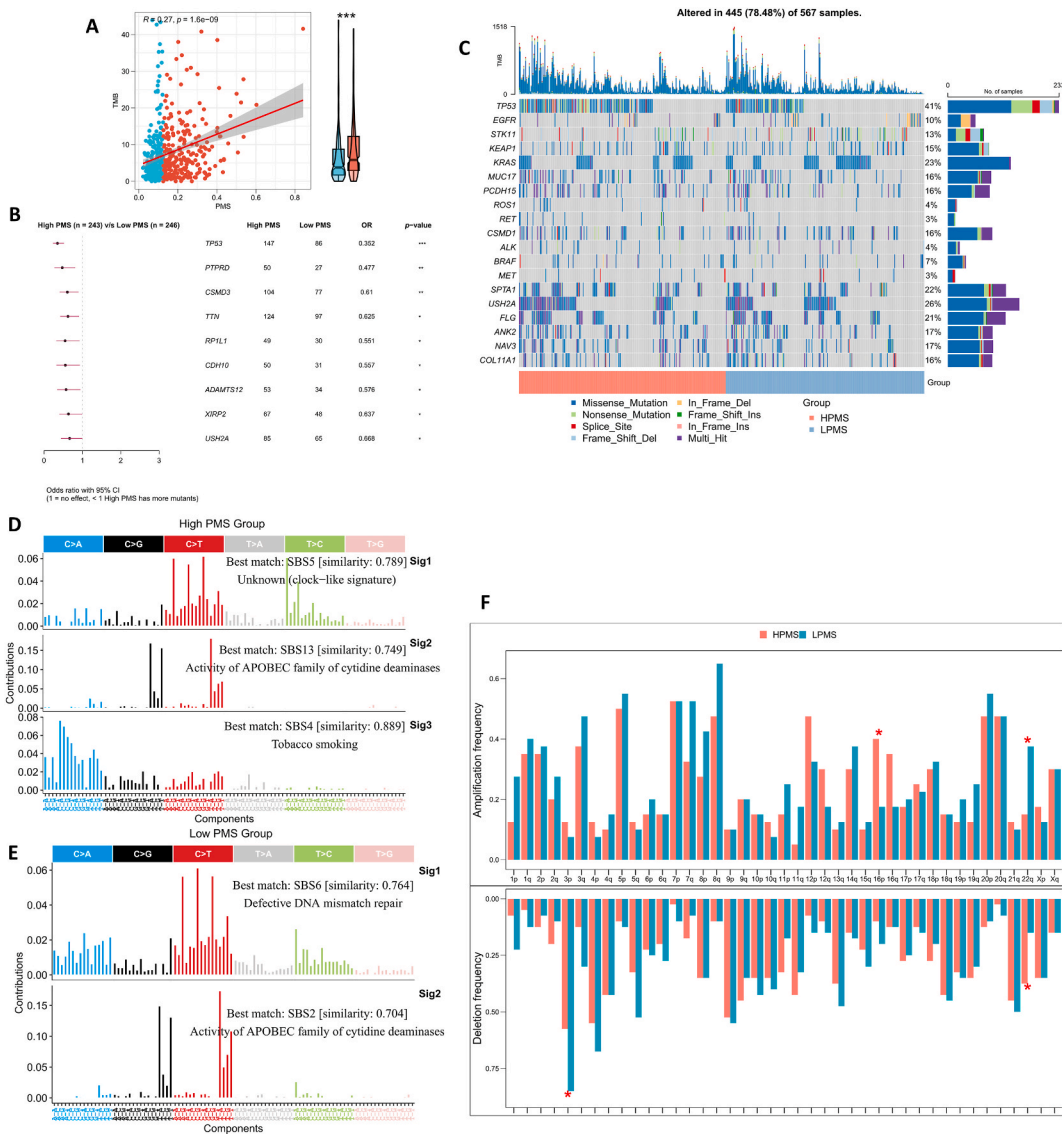
Fig. 6. PMS can distinguish genomic variation patterns in LUAD patients (A) Correlation of PMS and TMB. (B) The forest plot shows significantly mutated driver oncogenes among different PMS subgroups. (C) Oncoplot showing the mutation landscape of driver oncogenes among different PMS subtypes. (D) The NMF algorithm identified 3 mutant features in the high PMS group. (E) The NMF algorithm identified 2 mutant features in the low PMS group. (F) CNV differences between different PMS subgroups on the chromosome arms.

with high PMS (Fig. 6A). Furthermore, we found substantial differences in 9 high frequency mutated genes including TP53 between PMS subgroups (Fig. 6B). Oncoplot revealed the mutation profiles of all 25 high-frequency mutated genes between subgroups (Fig. 6C). Subsequently, three mutational features were identified in the high PMS as well as two in the low PMS group by the NMF algorithm (Fig. 6 D, E). APOBEC-related features (SBS2 and SBS13) played a dominant role in both groups. Notably, a significant smoking-related feature (SBS4) and an unknown SBS5 feature (Fig. 6D) were found in the high PMS group, while a dominant Defective DNA mismatch repair feature (SBS6) was found in the low PMS group (Fig. 6E). Subsequently, we determined that the high PMS group possessed higher amplification at 16p and higher deletion at 22q. While the low PMS group had more amplification on 22q and more deletions on 3p (Fig. 6F).

3.7. Patients having low PMS possess increased sensitivity to chemotherapy

Considering the variations in CNV and biological function among patients with PMS, we hypothesized that PMS could predict the response to chemotherapy in LUAD patients. First, we evaluated the IC50 of widely utilized chemotherapeutic agents for LUAD in different PMS groups relying on the GDSC database, and the findings yield that patients with low PMS possess increased sensitivity to four drugs (Cisplatin, Docetaxel, Doxorubicin, and Paclitaxel) (Fig. 7A). In contrast, patients with low PMS in the validation cohort possess increased sensitivity to Docetaxel and Paclitaxel (Fig. 7B). We therefore speculated that low PMS is more sensitive to Docetaxel and Paclitaxel. Potential drug targets highly associated with PMS and corresponding small molecule compounds may provide new chemotherapeutic options for high-risk LUAD patients. Therefore, using the median tau score as a guide, we identified 10 small molecule compounds that target high-risk PMS patients by submitting the Top 150 DEGs between low and high PMS subgroups to the
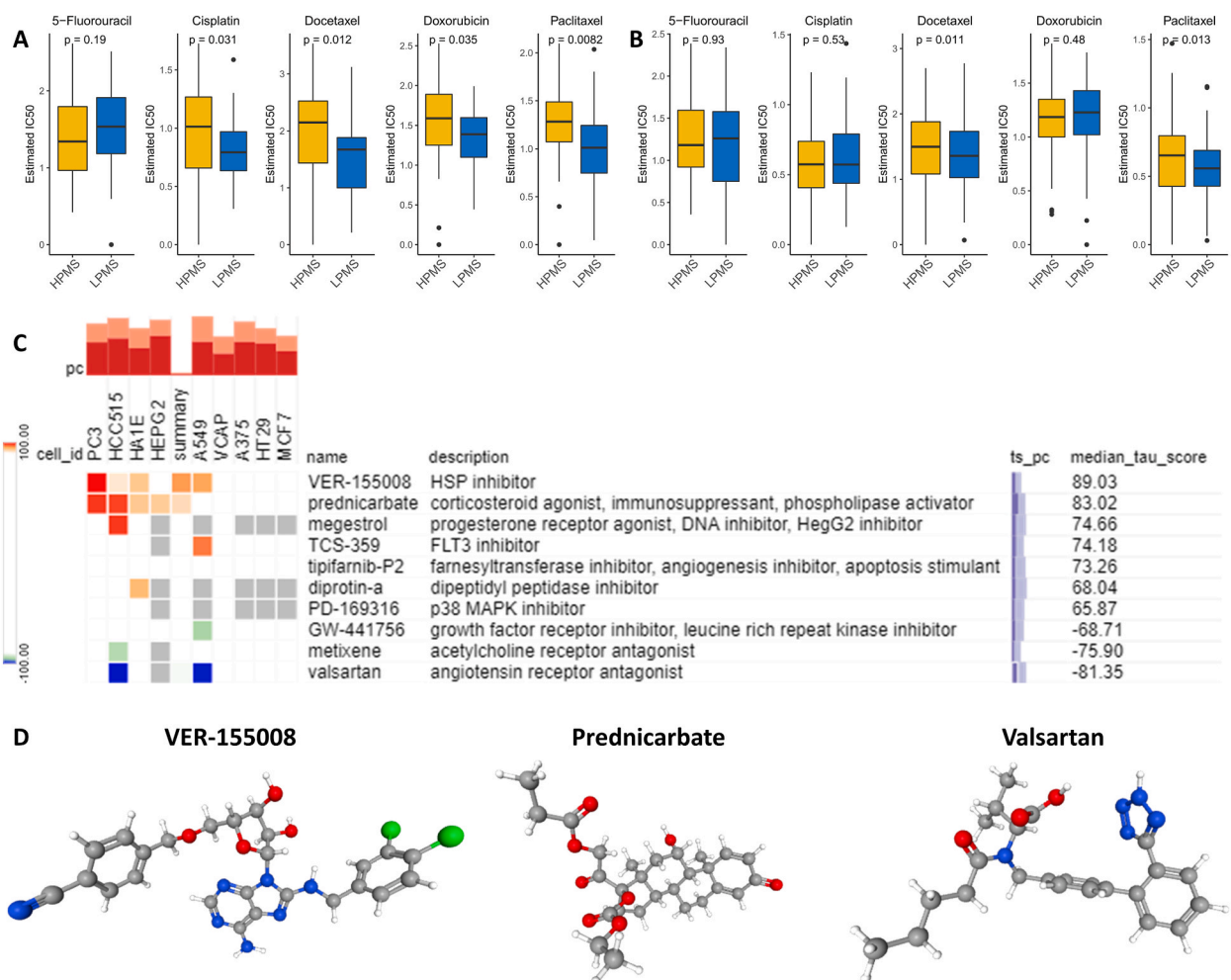
Fig. 7. PMS can predict chemotherapy The IC50 values of the five commonly used drugs (Cisplatin, Docetaxel, Doxorubicin, and Paclitaxel) in the TCGA cohort (A) and GEO cohort (B) were predicted based on the GDSC database. (C) Prediction of PMS-related drug targets as well as targeted small molecule compounds from the CMap database. (D) 3D molecular structures of the three most prospective small molecule compounds (Ver-155008, Prednicarbate and Valsartan).

CMap database (Fig. 7C). Higher tau scores represent more appropriate chemotherapy agents for patients with high LMS. Among them, the dominant action was the HSP inhibitor. We also provide the 3D molecular structures of the three compounds with the highest tau scores (Ver-155008, Prednicarbate and Valsartan) (Fig. 7D).

3.8. Inferring immunotherapy response

We believed that the low PMS group was more susceptible to immunotherapy since they exhibited a stronger antitumor immune response. Upon calculating each patient's IPS, we discovered that those with lower PMS had higher IPSs (Fig. 8 A, B). Next, we demonstrated that patients who have low PMS in both cohorts possessed a greater rate of response to immunotherapy by predicting the immune checkpoint inhibitor response in patients in the TCGA and GEO cohorts via the TIDE algorithm (Fig. 8 C, D). Moreover, in the TCGA and GEO cohort, PMS was the best predictor of response to immunotherapy compared to other indicators (Fig. 8 E, F). Lastly, we constructed the PMS in the IMvigor210 cohort. Here, insignificant difference can be found in overall survival between the two subgroups (Fig. 8G). However, taking into account the delayed effect of immunotherapy, immune checkpoint inhibitors usually take several months to take effect [23,24]. We calculated the difference in survival after 3 months and found that patients who have high PMS experienced significantly worse survival (Fig. 8H). Plus, patients who have low PMS had significantly higher neoantigens and TMB (Fig. 8 I, J).

3.9. PGM2 is significantly associated with malignant phenotype in LUAD

We constructed LUAD cell lines (H1975 and A549) with low expression of PGM2 by two different siRNAs (Fig. 9A). We first determined the effect of PGM2 on the proliferative capacity of the LUAD cell line by colony formation assays. The findings demonstrated that knockdown of PGM2 substantially minimized the proliferation level of both LUAD cell lines (H1975 and A549) (Fig. 9B). We then performed Transwell experiments with or without the addition of matrix gel to figure out the influence of PGM2 on the LUAD cell line's ability for migration and invasion. The results realistically knocked down PGM2 not only inhibited the migratory ability of LUAD cell lines, but also inhibited the invasive ability (Fig. 9C). Lastly, we carried out a scratch-healing assay to confirm the effect of
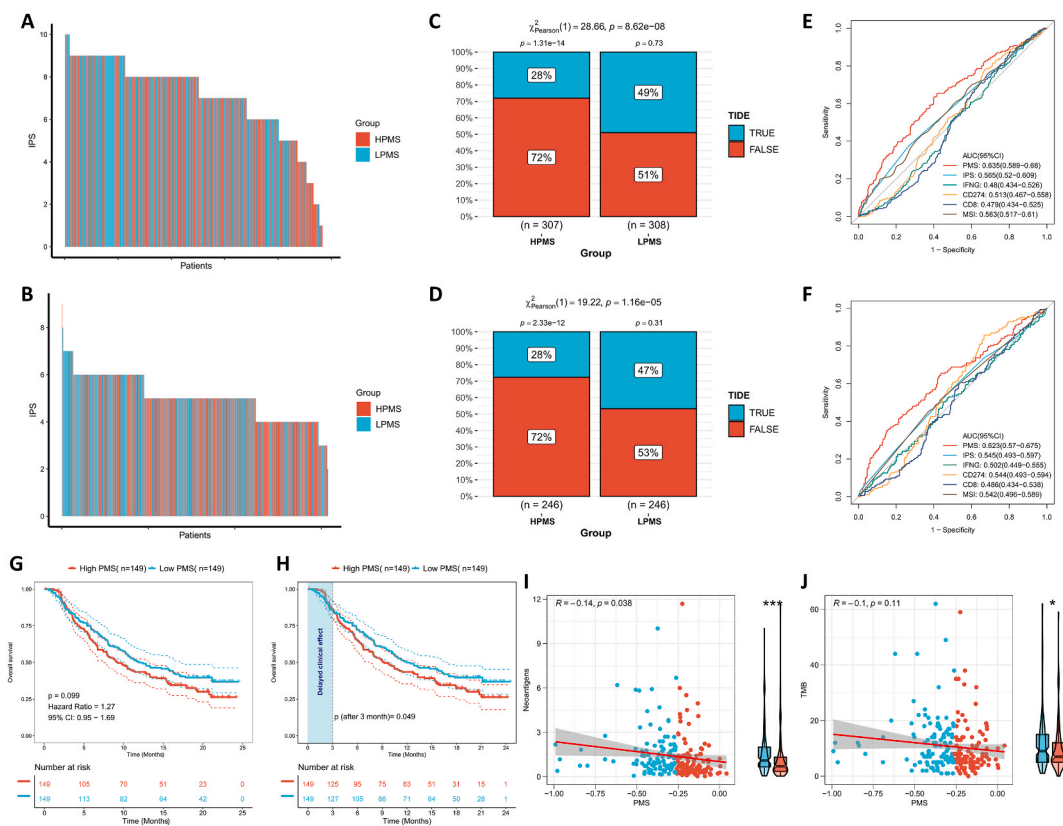
Fig. 8. PMS can predict immunotherapy The IPS of individual LUAD patients in the TCGA cohort (A) and GEO cohort (B). TIDE algorithm predicts response rates to immune checkpoint inhibitors for patients in the TCGA cohort (C) and GEO cohort (D). ROC curve shows the predictive efficiency for the response rate to immunotherapy by PMS and other indicators in the TCGA cohort (E) and GEO cohort (F). (G) KM survival curves for patients in the high- and low-PMS groups in IMvigor210 cohort. Scatter plot and box plot show the correlation of PMS with (H) neoantigens; (I) TMB in IMvigor210 cohort.
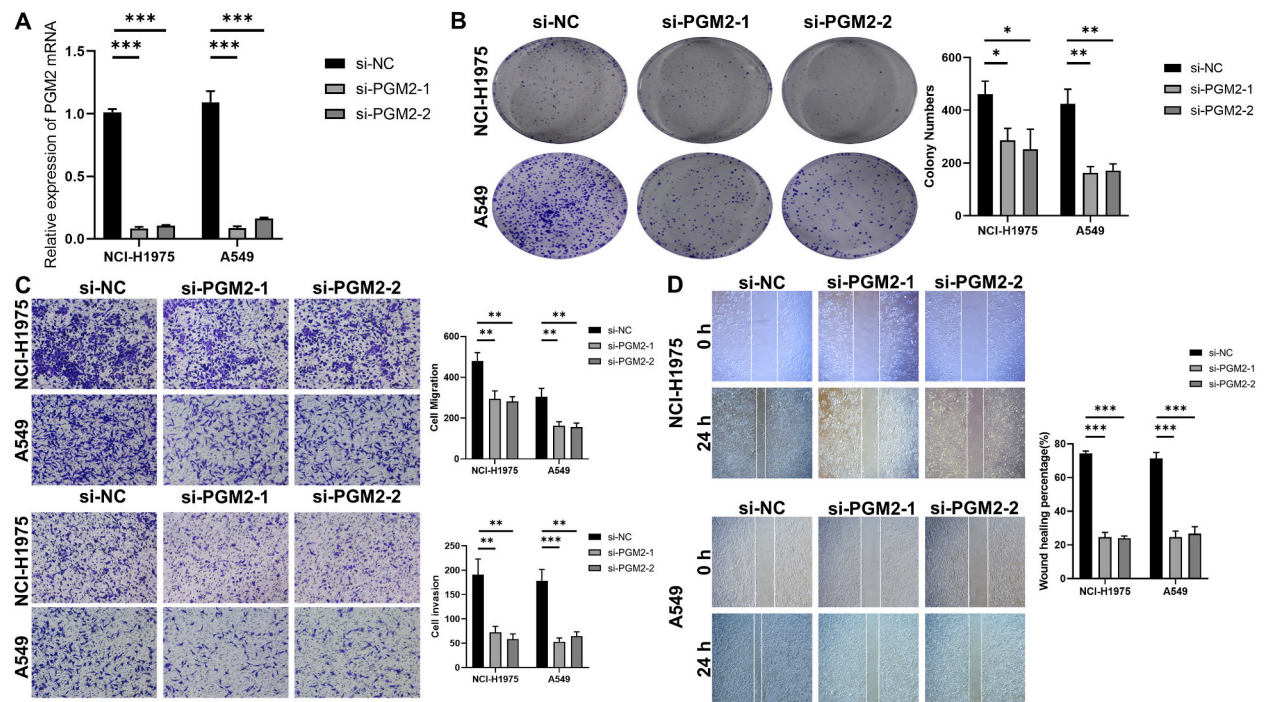
Fig. 9. Knockdown of PGM2 reduced the proliferation and invasion of LUAD cell lines (A) The knockout effect of si- **PGM2** was confirmed at the transcriptional level using qRT-PCR. (B)Representative images of colony formation in two lung cancer cell lines (H1975 and A549) after knockdown of PGM2 and their statistical results. (C) Representative images of Transwell assays in two lung cancer cell lines (H1975 and A549) after knockdown of PGM2 and their statistical results. Up: Migration assays; down: invasion assays. (D) Representative images of wound healing assays in two lung cancer cell lines after knockdown of PGM2 and their statistical results. Up: H1975 cell line; down: A549 cell line.

PGM2 on the migratory capacity of the LUAD cell line. The findings illustrated that the percentage of scratch healing after 24 h was lower in the LUAD cell line knocked down with PGM2 than in the control cell line (Fig. 9D).

4. Discussion

Lung cancer has been progressively becoming more common in recent years, especially in China [25]. LUAD is the main pathological type in patients with lung cancer, and advanced LUAD is extremely malignant and frequently has a bad prognosis as a result of treatment resistance [26–28]. Purine metabolism is crucial cancer progression and shows potential for application in immunotherapy. Pertaining to this particular research, we analyzed the transcriptome data of TCGA-LUAD and identified the core purine metabolism genes systematically. We identified a total of 50 prognostic purine metabolism genes. A significant positive correlation was discovered between them, which suggests the possibility of mutual regulation. Except for VCAN, the major regulation of all the core genes was CNV. Founded on these 18 core genes, we developed a 2-gene purine metabolism score (PMS) model by stepwise cox regression. We verified that PMS performs well across various LUAD cohorts and is a strong OS predictor in LUAD patients.

The dynamic processes of purine metabolism in tumors have a role in the tumor cells' proliferation and metastasis, and we then tried to understand the biological logic behind PMS. We discovered that the genes upregulated in samples from the high PMS group were primarily involved in cytoskeleton and collagen fiber formation. This suggests that high PMS is associated with more extracellular matrix (ECM) production [29]. More ECM also supported and promoted the growth of tumor cells, which may have led to a worse prognosis [30]. In addition, cell cycle, P53, RNA degradation, and other cell cycle pathways were more abundant in the high PMS group, suggesting the tumor cells in the group with higher PMS were more active in replication and proliferation and more malignant [31]. In contrast, the primary genes linked to the low PMS group's upregulation were immune response as well as cytokine pathways. More interestingly, the antigen-presentation pathway, hematopoietic cell lineage, as well as NK cell-mediated cell killing pathway were enriched in the low PMS group. Here, these particular outcomes imply that low PMS is associated with activation of the immune microenvironment, which may lead to more powerful antitumor immunity and improved prognosis for those in the low PMS category.

We tried to discuss in more depth the activated immune microenvironment in the low PMS group, Consequently, we looked at the two groups' differences from a variety of angles, such as immune pathways, immune cell infiltration, as well as immune checkpoints. The ESTIMATE results indicated that the low PMS group possessed greater immune scores, whereas the high PMS group possessed higher tumor purity. As mentioned previously, this may be due to the active proliferation of tumor cells in high PMS. We subsequently found increased expression of CD8A, LAG-3, as well as PD-1 in the low PMS group, indicating that immune checkpoint inhibitor treatment may be more appropriate for patients who have lower levels of PMS [32]. Additionally, we discovered that most

immune-related pathways were substantially upregulated in the low PMS group, suggesting a more robust and active anti-tumor immune response in the PMS group, which supports the results of our functional analysis. Notably, a worse prognosis may have resulted from the high PMS group's considerably greater Treg cell infiltration, which may have repressed the immune microenvironment and antitumor immune response [33].

We then examined genome-wide data to explore how genomic variations in PMS differ among individual patients, considering the crucial role of genomic alterations in tumor progression and the response to treatment, particularly in the context of immunotherapy. However, the small sample size may have contributed to our inability to find any substantial differences between the two groups' TMB and single nucleotide variants. For mutational signatures, the low PMS group possessed more SBS2 and SBS6, while the high PMS group had more SBS4, SBS5, and SBS13. The common feature shared by both groups was the APOBEC family (SBS2 and SBS13), which has been shown to be significant in LUAD patients in eight countries [34]. Our study reconfirms the specificity of APOBEC features in LUAD. Interestingly, we found significant smoking-related features in high PMS, which are linked to a higher incidence of lung cancer [35]. Finally, in the high PMS group, we discovered more CNV events. CNV has demonstrated to be a key component in gene regulation that modifies drug response and metabolism, ultimately causing treatment failure and disease recurrence by expediting the emergence of anticancer drug resistance [36,37]. Therefore, we infer that patients who have high PMS are resistant to chemotherapy and patients who have low PMS are suitable for chemotherapy.

Using information on drug sensitivity from three databases, we were able to confirm that patients with high PMS were resistant to chemotherapy. As per the GDSC database, we discovered that patients who have lower PMS were more susceptible to the effects of Docetaxel and Paclitaxel. Furthermore, by employing PMS to identify high-risk LUAD patients, we screened for potential drug targets and discovered corresponding small molecule compounds. Lastly, we determined the three small molecule compounds that are most likely to exist: VER-155008, Prednicarbate and Valsartan, which target the HSP, Corticosteroid and Angiotension pathways.

Lastly, we hypothesized that patients who have low PMS would respond better to immunotherapy from a variety of viewpoints. Firstly, IPS was higher in LUAD patients who have low PMS, which indicates that these patients might respond better to immunotherapy. Furthermore, patients with lower PMS also responded more frequently to immune checkpoint inhibitors (for instance, anti-PD-L1, anti-PD-1, and anti-CTLA-4) according to the TIDE algorithm. Additionally, PMS was a better predictor of immunotherapy response than conventional measures. Additionally, a cohort for external validation supported these findings. Despite this, no significant difference in the two groups' overall survival rates could be discovered. However, immunotherapy is generally considered to have a delayed effect, and the therapeutic effect is not evident at the beginning of the drug administration [23,24]. Therefore, we calculated the survival rate after 3 months of treatment for both groups and were surprised to discover that the survival rate of patients in the low PMS group was significantly higher than that of patients in the high PMS group. Additionally, we discovered a negative correlation between PMS and TMB and neoantigens, which could account for the improved prognosis of immunotherapy patients with low PMS [38,39].

There are still a few limitations on this research. Due to the dearth of data in this area, the study only includes two complete RNA-seq data sets for LUAD. In order to further corroborate our findings, we intend to gather more sequence or platform data for LUAD in the future. Furthermore, since we only concentrate on a small subset of mRNAs in the broad field of genomic regulation, we might have missed some other regulatory genomic data. Ultimately, it is unclear how the PMS influences biological processes and phenotypes. Nevertheless, we incorporated the functional enrichment analysis data to generate plausible conjectures, serving as motivation for further mechanistic research.

5. Conclusion

Pertaining to this particular research, we determined the possible crosstalk between purine metabolism of LUAD patients and established an PMS model to measure the level of the purine metabolism pathways. Patients with lower PMS possess a better prognosis and increased sensitivity to chemotherapy and immunotherapy. This finding is not only an addition to the existing field of cancer genomics but also offers novel approaches to the clinical management of LUAD and novel immunotherapy protocols.

Data availability statement

The research's original contributions have been incorporated in the article and supplemental material; for additional information, contact the corresponding author.

CRediT authorship contribution statement

Tingting Zhang: Writing – original draft. **Ruhua Chen:** Formal analysis. **Xiangyu Su:** Resources. **Meng Wang:** Validation. **Qin Lu:** Writing – review & editing.

Declaration of competing interest

The authors declare that they have no known competing financial interests or personal relationships that could have appeared to influence the work reported in this paper.

Acknowledgment

Appendix A. Supplementary data

Supplementary data to this article can be found online at https://doi.org/10.1016/j.heliyon.2024.e29290.

References

[1] N. Wang, C. Yu, T. Xu, D. Yao, L. Zhu, Z. Shen, et al., Self-assembly of DNA nanostructure containing cell-specific aptamer as a precise drug delivery system for cancer therapy in non-small cell lung cancer, J. Nanobiotechnol. 20 (1) (2022) 486, https://doi.org/10.1186/s12951-022-01701-5.

[2] L.A. Godoy, J. Chen, W. Ma, J. Lally, K.A. Toomey, P. Rajappa, et al., Emerging precision neoadjuvant systemic therapy for patients with resectable non-small cell lung cancer: current status and perspectives, Biomark. Res. 11 (1) (2023) 7, https://doi.org/10.1186/s40364-022-00444-7.

[3] R.L. Siegel, K.D. Miller, H.E. Fuchs, A. Jemal, Cancer statistics, 2021, CA A Cancer J. Clin. 71 (1) (2021) 7–33, https://doi.org/10.3322/caac.21654.

[4] J.S. Temel, L.A. Petrillo, J.A. Greer, Patient-centered palliative care for patients with advanced lung cancer, J. Clin. Oncol. : official journal of the American Society of Clinical Oncology 40 (6) (2022) 626–634, https://doi.org/10.1200/jco.21.01710.

[5] X. Lin, R. Ye, Z. Li, B. Zhang, Y. Huang, J. Du, et al., KIAA1429 promotes tumorigenesis and gefitinib resistance in lung adenocarcinoma by activating the JNK/MAPK pathway in an m(6)A-dependent manner, Drug Resist. Updates : reviews and commentaries in antimicrobial and anticancer chemotherapy 66 (2023) 100908, https://doi.org/10.1016/j.drup.2022.100908.

[6] K.A. Higgins, S. Puri, J.E. Gray, Systemic and radiation therapy approaches for locally advanced non-small-cell lung cancer, J. Clin. Oncol. : official journal of the American Society of Clinical Oncology 40 (6) (2022) 576–585, https://doi.org/10.1200/jco.21.01707.

[7] F. Cortiula, B. Reymen, S. Peters, P. Van Mol, E. Wauters, J. Vansteenkiste, et al., Immunotherapy in unresectable stage III non-small-cell lung cancer: state of the art and novel therapeutic approaches, Ann. Oncol. : official journal of the European Society for Medical Oncology 33 (9) (2022) 893–908, https://doi.org/10.1016/j.annonc.2022.06.013.

[8] X. Li, L. Zhang, T. Li, S. Li, W. Wu, L. Zhao, et al., Abplatin((IV)) inhibited tumor growth on a patient derived cancer model of hepatocellular carcinoma and its comparative multi-omics study with cisplatin, J. Nanobiotechnol. 20 (1) (2022) 258, https://doi.org/10.1186/s12951-022-01465-y.

[9] F. Di Virgilio, Purines, purinergic receptors, and cancer, Cancer Res. 72 (21) (2012) 5441–5447, https://doi.org/10.1158/0008-5472.Can-12-1600.

[10] E. Shoshan, A.K. Mobley, R.R. Braeuer, T. Kamiya, L. Huang, M.E. Vasquez, et al., Reduced adenosine-to-inosine miR-455-5p editing promotes melanoma growth and metastasis, Nat. Cell Biol. 17 (3) (2015) 311–321, https://doi.org/10.1038/ncb3110.

[11] J. Yin, W. Ren, X. Huang, J. Deng, T. Li, Y. Yin, Potential mechanisms connecting purine metabolism and cancer therapy, Front. Immunol. 9 (2018) 1697, https://doi.org/10.3389/fimmu.2018.01697.

[12] R.D. Leone, L.A. Emens, Targeting adenosine for cancer immunotherapy, Journal for immunotherapy of cancer 6 (1) (2018) 57, https://doi.org/10.1186/s40425-018-0360-8.

[13] D. Boison, G.G. Yegutkin, Adenosine metabolism: emerging concepts for cancer therapy, Cancer Cell 36 (6) (2019) 582–596, https://doi.org/10.1016/j.ccell.2019.10.007.

[14] W.B. Parker, Enzymology of purine and pyrimidine antimetabolites used in the treatment of cancer, Chem. Rev. 109 (7) (2009) 2880–2893, https://doi.org/10.1021/cr900028p.

[15] M.S. Schröder, A.C. Culhane, J. Quackenbush, B. Haibe-Kains, survcomp: an R/Bioconductor package for performance assessment and comparison of survival models, Bioinformatics 27 (22) (2011) 3206–3208, https://doi.org/10.1093/bioinformatics/btr511.

[16] A.M. Newman, C.L. Liu, M.R. Green, A.J. Gentles, W. Feng, Y. Xu, et al., Robust enumeration of cell subsets from tissue expression profiles, Nat. Methods 12 (5) (2015) 453–457, https://doi.org/10.1038/nmeth.3337.

[17] K. Yoshihara, M. Shahmoradgoli, E. Martínez, R. Vegesna, H. Kim, W. Torres-Garcia, et al., Inferring tumour purity and stromal and immune cell admixture from expression data, Nat. Commun. 4 (2013) 2612, https://doi.org/10.1038/ncomms3612.

[18] A. Mayakonda, D.C. Lin, Y. Assenov, C. Plass, H.P. Koeffler, Maftools: efficient and comprehensive analysis of somatic variants in cancer, Genome Res. 28 (11) (2018) 1747–1756, https://doi.org/10.1101/gr.239244.118.

[19] S. Wang, H. Li, M. Song, Z. Tao, T. Wu, Z. He, et al., Copy number signature analysis tool and its application in prostate cancer reveals distinct mutational processes and clinical outcomes, PLoS Genet. 17 (5) (2021) e1009557, https://doi.org/10.1371/journal.pgen.1009557.

[20] P. Geeleher, N. Cox, R.S. Huang, pRRophetic: an R package for prediction of clinical chemotherapeutic response from tumor gene expression levels, PLoS One 9 (9) (2014) e107468, https://doi.org/10.1371/journal.pone.0107468.

[21] P. Charoentong, F. Finotello, M. Angelova, C. Mayer, M. Efremova, D. Rieder, et al., Pan-cancer immunogenomic analyses reveal genotype-immunophenotype relationships and predictors of response to checkpoint blockade, Cell Rep. 18 (1) (2017) 248–262, https://doi.org/10.1016/j.celrep.2016.12.019.

[22] P. Jiang, S. Gu, D. Pan, J. Fu, A. Sahu, X. Hu, et al., Signatures of T cell dysfunction and exclusion predict cancer immunotherapy response, Nat. Med. 24 (10) (2018) 1550–1558, https://doi.org/10.1038/s41591-018-0136-1.

[23] E.L. Korn, B. Freidlin, Interim futility monitoring assessing immune therapies with a potentially delayed treatment effect, J. Clin. Oncol. : official journal of the American Society of Clinical Oncology 36 (23) (2018) 2444–2449, https://doi.org/10.1200/jco.2018.77.7144.

[24] V. Anagnostou, M. Yarchoan, A.R. Hansen, H. Wang, F. Verde, E. Sharon, et al., Immuno-oncology trial endpoints: capturing clinically meaningful activity, Clin. Cancer Res. : an official journal of the American Association for Cancer Research 23 (17) (2017) 4959–4969, https://doi.org/10.1158/1078-0432.Ccr-16-3065.

[25] P. Chen, Y. Liu, Y. Wen, C. Zhou, Non-small cell lung cancer in China, Cancer Commun. 42 (10) (2022) 937–970, https://doi.org/10.1002/cac2.12359.

[26] D. de Miguel-Perez, F.G. Ortega, R.G. Tejada, A. Martínez-Única, C.B. Peterson, A. Russo, et al., Baseline extracellular vesicle miRNA-30c and autophagic CTCs predict chemoradiotherapy resistance and outcomes in patients with lung cancer, Biomark. Res. 11 (1) (2023) 98, https://doi.org/10.1186/s40364-023-00544-y.

[27] Y. Hu, Y. Xu, T. Zhang, Q. Han, L. Li, M. Liu, et al., Cisplatin-activated ERβ/DCAF8 positive feedback loop induces chemoresistance in non-small cell lung cancer via PTEN/Akt axis, Drug Resist. Updates : reviews and commentaries in antimicrobial and anticancer chemotherapy 71 (2023) 101014, https://doi.org/10.1016/j.drup.2023.101014.

[28] X. Wang, Y. Li, R. Jin, X. Zheng, Y. Luo, P. Wu, et al., Single-cell analysis reveals the potential mechanisms of pyrotinib resistance in non-small cell lung cancer, Signal Transduct. Targeted Ther. 8 (1) (2023) 17, https://doi.org/10.1038/s41392-022-01226-1.

[29] R.S. Fischer, X. Sun, M.A. Baird, M.J. Hourwitz, B.R. Seo, A.M. Pasapera, et al., Contractility, focal adhesion orientation, and stress fiber orientation drive cancer cell polarity and migration along wavy ECM substrates, Proc. Natl. Acad. Sci. U.S.A. 118 (22) (2021), https://doi.org/10.1073/pnas.2021135118.

[30] X.Y. Yang, J.G. Zhang, Q.M. Zhou, J.N. Yu, Y.F. Lu, X.J. Wang, et al., Extracellular matrix modulating enzyme functionalized biomimetic Au nanoplatform-mediated enhanced tumor penetration and synergistic antitumor therapy for pancreatic cancer, J. Nanobiotechnol. 20 (1) (2022) 524, https://doi.org/10.1186/s12951-022-01738-6.

[31] H.K. Matthews, C. Bertoli, R.A.M. de Bruin, Cell cycle control in cancer, Nat. Rev. Mol. Cell Biol. 23 (1) (2022) 74–88, https://doi.org/10.1038/s41580-021-00404-3.

[32] S.L. Topalian, C.G. Drake, D.M. Pardoll, Immune checkpoint blockade: a common denominator approach to cancer therapy, Cancer Cell 27 (4) (2015) 450–461, https://doi.org/10.1016/j.ccell.2015.03.001.

[33] H. Nishikawa, S. Koyama, Mechanisms of regulatory T cell infiltration in tumors: implications for innovative immune precision therapies, Journal for immunotherapy of cancer 9 (7) (2021), https://doi.org/10.1136/jitc-2021-002591.

[34] S. Moody, S. Senkin, S.M.A. Islam, J. Wang, D. Nasrollahzadeh, R. Cortez Cardoso Penha, et al., Mutational signatures in esophageal squamous cell carcinoma from eight countries with varying incidence, Nat. Genet. 53 (11) (2021) 1553–1563, https://doi.org/10.1038/s41588-021-00928-6.

[35] H.G. Coleman, S.H. Xie, J. Lagergren, The epidemiology of esophageal adenocarcinoma, Gastroenterology 154 (2) (2018) 390–405, https://doi.org/10.1053/j.gastro.2017.07.046.

[36] Y. He, J.M. Hoskins, H.L. McLeod, Copy number variants in pharmacogenetic genes, Trends Mol. Med. 17 (5) (2011) 244–251, https://doi.org/10.1016/j.molmed.2011.01.007.

[37] L. Sansregret, B. Vanhaesebroeck, C. Swanton, Determinants and clinical implications of chromosomal instability in cancer, Nat. Rev. Clin. Oncol. 15 (3) (2018) 139–150, https://doi.org/10.1038/nrclinonc.2017.198.

[38] T.N. Schumacher, R.D. Schreiber, Neoantigens in cancer immunotherapy, Science (New York, N.Y.) 348 (6230) (2015) 69–74, https://doi.org/10.1126/science.aaa4971.

[39] T.A. Chan, M. Yarchoan, E. Jaffee, C. Swanton, S.A. Quezada, A. Stenzinger, et al., Development of tumor mutation burden as an immunotherapy biomarker: utility for the oncology clinic, Ann. Oncol. : official journal of the European Society for Medical Oncology 30 (1) (2019) 44–56, https://doi.org/10.1093/annonc/mdy495.